© 2016. Published by The Company of Biologists Ltd | Journal of Cell Science (2016) 129, 3320-3331 doi:10.1242/jcs.185223

RESEARCH ARTICLE

Apicoplast fatty acid synthesis is essential for pellicle formation at the end of cytokinesis in *Toxoplasma gondii*

Érica S. Martins-Duarte[1,2,*], Maira Carias[1,2], Rossiane Vommaro[1,2], Namita Surolia[3] and Wanderley de Souza[1,2,*]

ABSTRACT

The apicomplexan protozoan *Toxoplasma gondii*, the causative agent of toxoplasmosis, harbors an apicoplast, a plastid-like organelle with essential metabolic functions. Although the FASII fatty acid biosynthesis pathway located in the apicoplast is essential for parasite survival, the cellular effects of FASII disruption in *T. gondii* had not been examined in detail. Here, we combined light and electron microscopy techniques – including focused ion beam scanning electron microscopy (FIB-SEM) – to characterize the effect of FASII disruption in *T. gondii*, by treatment with the FASII inhibitor triclosan or by inducible knockdown of the FASII component acyl carrier protein. Morphological analyses showed that FASII disruption prevented cytokinesis completion in *T. gondii* tachyzoites, leading to the formation of large masses of 'tethered' daughter cells. FIB-SEM showed that tethered daughters had a mature basal complex, but a defect in new membrane addition between daughters resulted in incomplete pellicle formation. Addition of exogenous fatty acids to medium suppressed the formation of tethered daughter cells and supports the notion that FASII is essential to generate lipid substrates required for the final step of parasite division.

KEY WORDS: Cell division, Bradyzoite, Triclosan, Apicomplexa, Cleavage furrow

INTRODUCTION

Toxoplasma gondii is the protozoan responsible for toxoplasmosis, a disease with wide global distribution. *T. gondii* infects at least one third of the human population, although infection by this parasite is usually asymptomatic. However, *T. gondii* infection is one of the leading causes of mortality in immune-compromised patients, and is also associated with several congenital malformations, miscarriage and newborn ocular disease (when transmitted congenitally) (Montoya and Liesenfeld, 2004). Despite the medical importance of *T. gondii*, therapy against infections by this parasite is restricted to a limited number of drugs, which are effective only against the acute-stage tachyzoite form, and do not clear chronic infection by encysted bradyzoite forms. Thus, toxoplasmosis is a lifelong infection (McLeod et al., 2013).

T. gondii and other members of the phylum Apicomplexa – which includes the malaria agent *Plasmodium falciparum* – harbor an 'apicoplast', a non-photosynthetic secondary plastid originating from a red algae plastid that was engulfed by an apicomplexan ancestor (Williamson et al., 1994; Köhler et al., 1997). Besides the evolutionary importance of the apicoplast, its discovery brought new opportunities for the development of novel therapy targeting diseases caused by apicomplexan parasites (Wiesner et al., 2008; Goodman and McFadden, 2013). As in plant plastids, the apicoplast contains its own genome and pathways for the synthesis of isoprenoids, fatty acids and iron-sulfur (Fe-S) clusters (Sheiner et al., 2013; van Dooren and Striepen, 2013). More importantly, owing to the prokaryotic ancestry of the apicoplast, its pathways are divergent from the eukaryotic counterparts found in the mammalian host, which enables the development of selective compounds against the parasite that are less toxic towards the host (Wiesner et al., 2008; Goodman and McFadden, 2013).

The apicoplast machinery for fatty acid synthesis – the FASII fatty acid biosynthesis pathway – consists of a system of independent enzymes (encoded by different genes), each responsible for a distinct step during fatty acid chain elongation (Waller et al., 1998; White et al., 2005). This mechanism of fatty acid synthesis contrasts with that of the FASI pathway found in the mammalian host, and also in the cytoplasm of *T. gondii*, which consists of one large multifunctional polypeptide (White et al., 2005). During fatty acid synthesis by the FASII pathway, the growing fatty acyl radicals are bonded to the acyl carrier protein (ACP), and fatty acyl elongation consists of cyclic sequential reactions performed by the enzymes β-ketoacyl-ACP synthase, β-ketoacyl-ACP reductase, β-hydroxyacyl-ACP dehydratase and enoyl-ACP reductase (ENR) (White et al., 2005).

Although *T. gondii* obtains lipids from the host cell (Charron and Sibley, 2002; Quittnat et al., 2004; Bisanz et al., 2006), intracellular tachyzoites also synthesize several major fatty acids *de novo* (Ramakrishnan et al., 2012), and both the FASII and the endoplasmic reticulum fatty acid elongation pathway (ELO) (Mazumdar et al., 2006; Ramakrishnan et al., 2012, 2015) are essential for parasite survival. In contrast, the importance of the FASI pathway for parasite biology remains unclear.

Since the discovery of the FASII pathway in the apicoplast, the fate and importance of its products for parasite lipid metabolism and survival have been extensively studied (Mazumdar et al., 2006; Yu et al., 2008; Vaughan et al., 2009; Ramakrishnan et al., 2012). Treatment with FASII inhibitors (Zuther et al., 1999; McLeod et al., 2001; Waller et al., 2003) and conditional depletion of the FASII component ACP (Mazumdar et al., 2006) leads to parasite growth impairment, both *in vitro* and *in vivo*. Indeed, induction of ACP knockdown also causes an apicoplast segregation defect (Mazumdar et al., 2006). In *T. gondii* FASII is responsible for the synthesis of over 80% of the saturated long-chain fatty acids (LCFA) C14:0 and C16:0, and its disruption remarkably reduced the synthesis of saturated LCFA with up to 18 carbons (Ramakrishnan, et al., 2012). High levels of LCFA are also found in

[1]Laboratório de Ultraestrutura Celular Hertha Meyer, Instituto de Biofísica Carlos Chagas Filho, Universidade Federal do Rio de Janeiro, Rio de Janeiro, Brazil, 21.941-902. [2]Instituto Nacional de Ciência e Tecnologia em Biologia Estrutural e Bioimagens, Rio de Janeiro, Brazil, 21.941-902. [3]Molecular Biology and Genetics Unit, Jawaharlal Nehru Centre for Advanced Scientific Research, Jakkur, Bangalore, India, 560064.

*Authors for correspondence (erica@biof.ufrj.br; wsouza@biof.ufrj.br)

É.S.M.-D., 0000-0003-0925-6953

Received 21 December 2015; Accepted 19 July 2016

Journal of Cell Science

Journal of Cell Science (2016) 129, 3320-3331 doi:10.1242/jcs.185223

phosphatidylcholine, a major phospholipid in *T. gondii* (Welti et al., 2007). Parasite proliferation after disruption of the FASII pathway can be partially rescued by adding myristate (C14:0) and palmitate (C16:0) to the growth medium, which shows that FASII LCFA products are essential for *T. gondii* (Ramakrishnan et al., 2012). A proportion of FASII LCFAs is used as precursors for the synthesis of very long chain fatty acid (VLCFA) by the ELO pathway (Ramakrishnan et al., 2012). Also, FASII is essential for providing octanoic acid, a precursor for the synthesis of lipoic acid, an important cofactor for the apicoplast pyruvate dehydrogenase (Thomsen-Zieger et al., 2003; Crawford et al., 2006; Mazumdar et al., 2006).

Although molecular and biochemical aspects of the FASII pathway have been dissected, the phenotypic consequences of FASII disruption for *T. gondii* cells have not been examined in detail in order to clarify the role of FASII products for *T. gondii* parasite biology. Here, we examined the effect of FASII inhibition on *T. gondii* tachyzoites, by performing a detailed light and electron microscopy analysis of parasites subjected to pharmacological and genetic FASII disruption. Pharmacological FASII inhibition was accomplished by treatment of infected cells with triclosan, a well-characterized inhibitor of the FASII enzyme ENR (Heath et al., 1998). Triclosan is widely used as an anti-bacterial agent in consumer products and its antiproliferative effect against *T. gondii in vitro* has been reported previously (McLeod et al., 2001). Genetic FASII disruption was accomplished using a tetracycline-inducible ACP mutant (Mazumdar et al., 2006). Our data show that FASII is essential for the completion of *T. gondii* cytokinesis, which explains the anti-proliferative effect of FASII inhibition on this parasite.

RESULTS

Triclosan treatment triggers stage conversion of *T. gondii* tachyzoites

As an initial strategy to evaluate the phenotypic effect of FASII disruption in *T. gondii*, we used the antibiotic triclosan, a well-characterized inhibitor of the FASII enzyme ENR, the final (and regulatory) step in FASII (Heath et al., 1998; Heath and Rock, 1995), whose localization in the apicoplast was confirmed by antibody labeling (Ferguson et al., 2005).

Triclosan has antiproliferative effect against *T. gondii* tachyzoites and other apicomplexans (McLeod et al., 2001; Surolia and Surolia, 2001; Bork et al., 2003). We made dose–response curves for *T. gondii* tachyzoites grown *in vitro*, in LLC-MK$_2$ cells. The IC$_{50}$ values calculated for the growth curves obtained after 24 and 48 h of treatment were 0.83 µg/ml and 0.24 µg/ml, respectively (Fig. S1A). Based on the dose–response curves, we selected for further study a concentration of 1 µg/ml triclosan, which inhibited 56% and 70% of the tachyzoite proliferation after 24 and 48 h of treatment, respectively, and also used 0.5 µg/ml triclosan as an intermediate concentration.

To verify whether the inhibitory effect of triclosan against *T. gondii* was able to eradicate the infection, we performed plaque assays where confluent monolayers of human foreskin fibroblasts (HFFs) were infected with tachyzoites of *T. gondii* and then treated for 2 or 5 days with 1.0 µg/ml of the drug. After treatment, infected cells were allowed to proliferate for an additional 8 days in medium without the drug. Infected cultures treated with 0.5 or 1.0 µg/ml of triclosan for 2 days contained smaller and less numerous plaques compared with untreated cultures (Fig. S1B–D), the number and size of plaques in infected cultures was compatible with 65% and 70% tachyzoite growth inhibition, respectively, in agreement with the dose–response curves (Fig. S1C,D). However, small plaques containing parasites were observed even after 5 days of treatment with 1.0 µg/ml of triclosan (circled area in Fig. S1B and arrowheads in inset), indicating residual infection.

Considering that the cystic bradyzoite stage of *T. gondii* is naturally refractory to drug treatments (McLeod et al., 2013), we evaluated whether triclosan treatment induced the conversion of tachyzoites into bradyzoites. Cultures infected with tachyzoites were treated for 2 and 5 days with 0.5 or 1.0 µg/ml of triclosan, and then labeled with an antibody against the tachyzoite surface protein SAG1 and with the lectin DBA, which recognizes the bradyzoite cyst wall component N-acetylgalactosamine (Zhang et al., 2001). In untreated cells, few parasitophorous vacuoles were positive for DBA–FITC, whereas treatment with triclosan for 2 or 5 days resulted in a significant increase in the number of vacuoles labeled for DBA–FITC, or double-labeled with anti-SAG1 antibody and DBA–FITC (Fig. S1E, $P<0.05$ one-way ANOVA). The conversion of tachyzoites into bradyzoites was also confirmed by thin-section transmission electron microscopy (TEM) analysis of infected cells treated with 1 µg/ml triclosan for 48 h, which showed parasites with amylopectin granules (asterisks in Fig. S1F) inside vacuoles of increased density (arrow in Fig. S1F); both features are indicative of stage conversion (Ferguson and Hutchison, 1987).

Triclosan treatment affects *T. gondii* cell division

Considering that FASII ACP knockdown causes apicoplast loss and defects in its morphology and biogenesis along the *T. gondii* division cycle (Mazumdar et al., 2006), we investigated whether triclosan treatment also caused an apicoplast inheritance defect, in association with the cell division. For that we labeled infected cells with antibodies against the inner membrane complex (IMC) (anti-IMC1, in red), a marker for daughter cell boundaries and the mother cell pellicle, and the apicoplast (anti-HSP60, in green) (Fig. 1).

T. gondii tachyzoites divide by 'endodyogeny', which consists of the formation of two new daughter cells inside a single mother cell (Goldman et al., 1958; Sheffield and Melton, 1968). During this process the IMC, which provides a scaffold for daughter cell budding, is formed *de novo*. The IMC is composed of flattened membranous sacs (the alveoli) delimited by two unit membranes and by a filamentous network that covers the cytoplasmic side of the alveoli and is associated to the subpellicular microtubules (Porchet and Torpier, 1977; Dubremetz and Torpier, 1978; Morrissette et al., 1997). Mitosis and the partition of organelles such as the apicoplast occur while daughter cells bud inside the mother. At the end of cytokinesis, the two new daughter cells emerge and leave behind remnant residual body (Sheffield and Melton, 1968; Nishi et al., 2008).

Untreated tachyzoites were arranged in the typical 'rosette' organization after 24 h of infection, with individualized parasites containing just one apicoplast each (Fig. 1A). However, treatment of tachyzoites with concentrations as low as 0.5 µg/ml triclosan for 24 h (i.e. below the IC$_{50}$) led not just to alterations in apicoplast morphology and inheritance, but also to a cell division defect (Fig. 1B). Treatment with 0.5 µg/ml caused incorrect inheritance of the apicoplast during endodyogeny, as we observed daughter cells devoid of an apicoplast (asterisks in Fig. 1B), due to missegregation of two apicoplasts to single daughter cells or to apicoplast positioning outside daughter cell boundaries (green arrows in Fig. 1B). After treatment with 0.5 µg/ml triclosan, we also observed incomplete parasite division, with 'tethered' daughter cells (arrow in Fig. 1B), and parasites often contained enlarged apicoplasts (arrowheads in Fig. 1B). Treatment with 1.0 µg/ml had a more drastic effect on the apicoplast and on cell division, leading to the

Journal of Cell Science (2016) 129, 3320-3331 doi:10.1242/jcs.185223

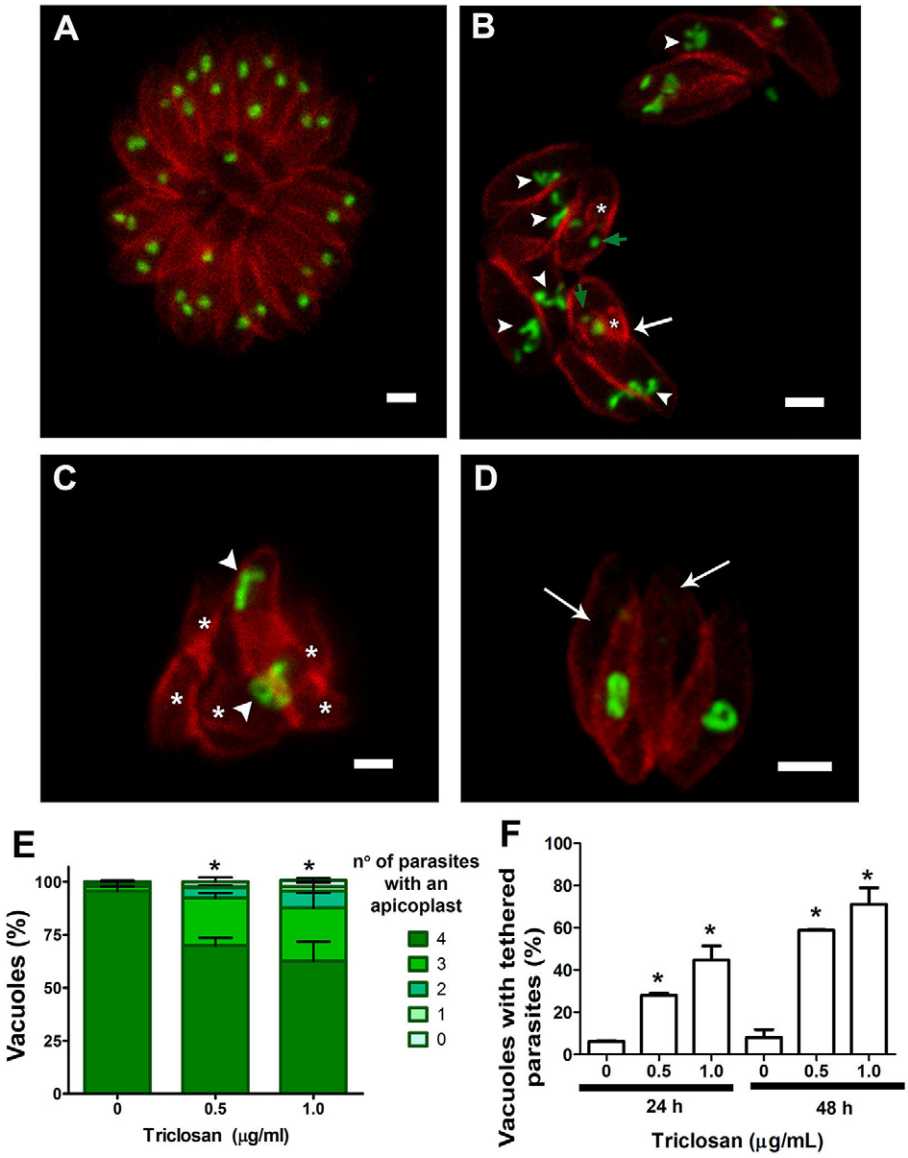

Fig. 1. Triclosan treatment affected apicoplast inheritance and parasite division. Immunofluorescence microscopy of *T. gondii* tachyzoites after treatment with 0.5 and 1.0 µg/ml of triclosan for 24 h, showing apicoplasts (in green, labeled with anti-HSP60 antibody) and tachyzoite membranes (in red, labeled with anti-IMC1 antibody). (A) Untreated parasites were typically organized in 'rosettes', and had apicoplasts of normal shape and size. (B) Tachyzoites treated with 0.5 µg/ml of triclosan had enlarged apicoplasts (arrowheads), signs of cell division defects (arrow), and clear signs of apicoplast missegregation defects (green arrows), including newly forming daughter cells devoid of this organelle (asterisks). (C) Treatment with 1 µg/ml triclosan led to the formation of masses of tethered daughter cells, some of which contained an enlarged apicoplast (arrowheads), whereas others were devoid of an apicoplast (asterisks). (D) Vacuole containing individual parasites devoid of an apicoplast (arrows). Scale bars: 2 µm. (E) Quantification of the number of parasites containing an apicoplast in vacuoles of four individual parasites, after treatment with 0.5 and 1 µg/ml of triclosan for 24 h (mean+s.d. of three independent experiments). (F) Quantification of parasitophorous vacuoles containing tethered parasites after treatment with 0.5 or 1 µg/ml of triclosan for 24 h and 48 h [mean+s.d. of three (24 h) and two (48 h) independent experiments]. **P*<0.05 compared to untreated (one-way ANOVA).

formation of complex masses of tethered daughter cells (Fig. 1C), some of which contained enlarged apicoplasts (arrowheads in Fig. 1C), while others were devoid of this organelle (asterisks in Fig. 1C). Individual (i.e. non-tethered) parasites without an apicoplast were also observed (arrow Fig. 1D). Quantification analysis of vacuoles containing four individual parasites after treatment with 0.5 and 1.0 µg/ml of triclosan for 24 h showed that ~30% of vacuoles contained at least one parasite devoid of an apicoplast (Fig. 1E; $P<0.05$, one-way ANOVA). Quantification of vacuoles containing tethered daughter cells (such as in Fig. 1B,C) showed that this defect was a consequence of triclosan treatment in *T. gondii*, with 0.5 and 1.0 µg/ml of triclosan resulting in 35% and 45% of vacuoles with tethered daughter cells, respectively, compared with <10% in the untreated control after 24 h (Fig. 1F; $P<0.05$, one-way ANOVA).

Triclosan treatment led to tachyzoite cytokinesis failure

To analyze the effect of triclosan on *T. gondii* morphology by TEM, LLC-MK$_2$ cells infected with tachyzoites were treated with 1 µg/ml of triclosan for 24 and 48 h. Triclosan treatment had a clear effect on the *T. gondii* division process (Fig. 2). Untreated parasites had the typical tachyzoite morphology and segregated as individual daughter cells during cell division by endodyogeny (Fig. 2A), whereas triclosan clearly interrupted *T. gondii* cytokinesis, at the end of endodyogeny. Daughter cells were able to complete mitosis (as evidenced by the presence of individual daughter nuclei) but could not completely bud from the mother cell, which led to the formation of tethered daughter cells (Fig. 2B–D). Although the division process was not completed, tethered daughter cells (arrow in Fig. 2B) were still able to start new rounds of endodyogeny, given that new daughter cell buds – identified by the presence of new IMC scaffolds – emerged inside tethered cells (arrowheads in Fig. 2B). We also observed multiple well-delimited tethered daughter cells (asterisks in Fig. 2C,D), each containing a single nucleus and displaying normal IMC morphology (with underlying subpellicular microtubules; arrowhead in inset from Fig. 2D).

Cytokinesis failure is an on-target effect of FASII disruption

Although triclosan has a strong inhibitory effect on the replication of the asexual blood stage of *Plasmodium* spp., the FASII pathway targeted by triclosan is not required for the replication of this stage of the parasite (Yu et al., 2008; Vaughan et al., 2009; Goodman

Journal of Cell Science

Journal of Cell Science (2016) 129, 3320-3331 doi:10.1242/jcs.185223

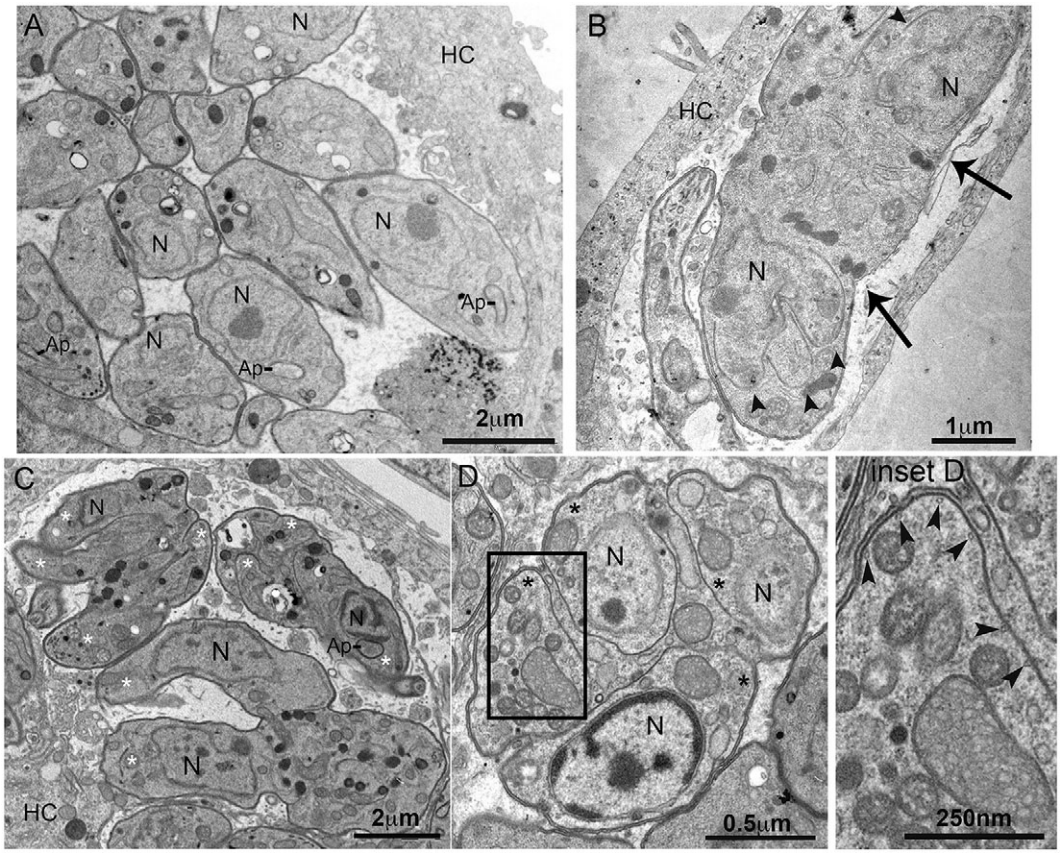

Fig. 2. TEM analysis of the effect of triclosan on *T. gondii* division. LLC-MK$_2$ cells were infected with *T. gondii* tachyzoites and then treated with 1 µg/ml of triclosan for 24 and 48 h. (A) Untreated tachyzoites showed normal morphology and division. (B) Image of an infected cell after 24 h of triclosan treatment, showing a parasitophorous vacuole containing two daughter cells still tethered by their basal ends (arrows), although new cycles of division have initiated (arrowheads indicate newly forming daughter cells). (C,D) Parasitophorous vacuoles of infected cells after 48 h of triclosan treatment, containing large parasites with tethered daughter cells (asterisks in C and D) displaying normal (IMC) morphology with underlying microtubules (arrowheads in inset for D). Ap, apicoplast; HC, host cell; N, nucleus.

et al., 2014). These data suggest that the effect of triclosan against apicomplexan parasites is 'off-target', rather than due to ENR inhibition and fatty acid synthesis disruption (Botté et al., 2012). However, the crystal structure of *T. gondii* and *P. falciparum* ENR in complex with NAD+ and triclosan, as well as an enzymatic assay *in vitro*, have shown a slow and tight binding kinetic similar to that observed for bacterial and plant ENR (Kapoor et al., 2004; Muench et al., 2007).

To confirm that the cytokinesis failure observed after triclosan treatment was caused by a bona fide on-target effect of FASII inhibition, we analyzed the phenotype of the tetracyclin-inducible mutant of the FASII component ACP (ΔACP/ACPi) (Mazumdar et al., 2006). The ΔACP/ACPi mutant was generated by stable transformation of the TAti tet-transactivator line of *T. gondii* with an ectopic minigene copy of ACP under the control of the tetracycline responsive ('tet-off') promoter 7tetOSag4, followed by the allelic replacement of the native ACP gene by a cassette containing the chloramphenicol acetyl transferase gene (for more information, see Mazumdar et al., 2006).

In line with results reported previously (Mazumdar et al., 2006), we observed apicoplast loss after ACP knockdown with anhydrous tetracylcin (Atc) in the mutant ΔACP/ACPi, and this defect became more pronounced at longer induction periods, with only 19% of the parasitophorous vacuoles containing all four parasites harboring an apicoplast, after 96 h of induction (Fig. 3A). Similar to results observed after triclosan treatment, genetic disruption of FASII function also caused a parasite division defect (Fig. 3B). As observed after treatment with triclosan, induction of ΔACP/ACPi resulted in parasitophorous vacuoles containing masses of tethered daughter cells (Fig. 3B), many of which were devoid of an apicoplast, after 72 and 96 h of induction (asterisks in Fig. 3B). Quantification of the number of vacuoles containing tethered parasites (Fig. 3C) confirmed that the appearance of tethered parasites was a major phenotype of FASII disruption after ACP knockdown by Atc. After 48 h of induction with Atc, the effect on cell division reached a plateau with ∼57% of parasitophorous vacuoles containing tethered parasites (Fig. 3C).

We also evaluated whether FASII fatty acid inhibition after ACP knockdown would increase the number of vacuoles showing conversion into the bradyzoite stage (Fig. 3D). As observed after triclosan treatment, knockdown of ACP after a 5-day induction period significantly increased the number of vacuoles labeled for DBA–FITC and double-labeled with anti-SAG1 antibody and DBA–FITC after 5 days (Fig. 3D; $P<0.05$, one-way ANOVA). By contrast, Atc treatment of an RH strain did not cause stage conversion of tachyzoites into bradyzoites (Fig. 3D).

TEM analysis of LLC-MK$_2$ cells infected with ΔACP/ACPi confirmed a pattern of division defects similar to that observed after triclosan treatment (Fig. 4). Although non-induced mutants showed a normal morphology and division (Fig. 4A), we observed cytokinesis failure after mutation induction with Atc for 48, 72 and 96 h (Fig. 4B–F), with the formation of groups of tethered

Journal of Cell Science (2016) 129, 3320-3331 doi:10.1242/jcs.185223

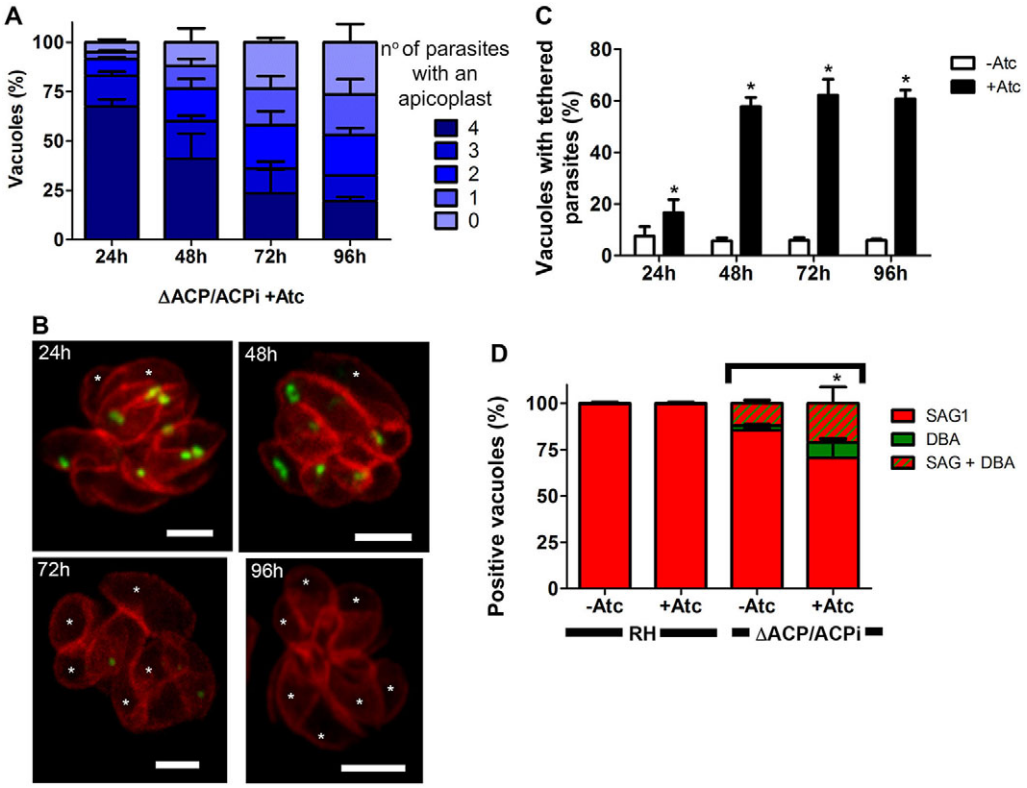

Fig. 3. Effect of FASII genetic disruption on parasite division and stage conversion. LLC-MK$_2$ cells were infected with the *T. gondii* ΔACP/ACPi mutant and then ACP knockdown was induced by treatment with (+Atc) or without (-Atc) anhydrous tetracycline. (A) Quantification of the number of tachyzoites containing an apicoplast in vacuoles of four individual parasites, after induction with Atc for 24–96 h (mean+s.d. of two independent experiments). (B) Immunofluorescence microscopy images of infected LLCMK$_2$ cells, showing parasite boundaries (labeled with anti-IMC1 antibody, in red) and apicoplasts (labeled with anti-HSP60 antibody, in green). Induction of ΔACP/ACPi with Atc for 24 to 96 h led to the formation of masses of tethered daughter cells and to apicoplast loss (asterisks). Scale bars: 2 µm. (C) Quantification of parasitophorous vacuoles with tethered tachyzoites (based on immunofluorescence data) after ΔACP/ACPi induction (mean+s.d. of three independent experiments). *P<0.05 compared to without Atc (Student's t-test). (D) Analysis of the conversion of tachyzoites into the cystic bradyzoite stage upon ACP knockdown, by labeling of infected cells with an anti-SAG1 antibody (to recognize tachyzoites) and with the lectin DBA–FITC, which recognizes a cyst wall component (mean+s.d. of three independent experiments). *P<0.05 compared to -Atc (Student's t-test). Cells infected with RH strain parasites were used as a negative control for ACP knockdown induction.

daughter cells. As observed for parasites treated with triclosan (Fig. 2), well-delimited tethered daughter cells within each group contained a single nucleus and a complete set of organelles, including a mitochondrion.

In agreement with the results that were observed after treatment with triclosan, induced mutants displayed normal IMC morphology, with the underlying microtubules (arrows in Fig. 4F), even though cytokinesis was incomplete. Large round masses of tethered parasites were observed after 72 and 96 h of treatment with Atc (Fig. 4C–E). Curiously, some tethered daughter cell masses contained vesicles between tethered daughters (arrowheads in Fig. 4B,E,F, and inset for B), which is reminiscent of cleavage furrow formation (Sheffield and Melton, 1968; Morrissette and Sibley, 2002), and might represent abortive cleavage furrows.

Tethered daughter cells have a mature basal complex, but an incomplete pellicle

To evaluate in more detail the extent of the cytokinesis defect observed after FASII disruption, we examined serial sections of the tethered junction between unseparated daughter cells using focused-ion beam scanning electron microscopy (FIB-SEM), after treatment of infected cells with 1.0 µg/ml of triclosan for 24 h (Movie 1 and Fig. 5), and ACP knockdown induction for 72 h (Movie 2 and Fig. 6).

The serial images of parasites after treatment with triclosan show an infected cell clearly containing two individual tachyzoites (parasites 1 and 3 in Fig. 5C–E) and two tethered daughter cells (parasites 2 and 4 in Fig. 5C–E) linked by their basal ends. Note that individual cells remained connected to neighboring tethered parasites through a small portion of their basal ends (arrow in Fig. 5B). This bond of a small portion of the basal end of daughter cells to the residual body (of the mother cell) is expected at this stage in the intracellular infection cycle (Sheffield and Melton, 1968) and is believed to contribute to parasite rosette organization (Muñiz-Hernandez et al., 2011), within the parasitophorous vacuole.

The apical body portion of tethered daughter cells had a fully formed pellicle, which consists of a trilaminar structure composed of the plasma membrane and the IMC double membrane (Vivier and Petitprez, 1969) (Fig. 5C,D). In contrast, the basal tethered region of daughter cells contained a large section of IMC (equivalent to about one quarter of the parasite circumference) not associated with a corresponding section of plasma membrane (brackets in Fig. 5C,D). This suggests that pellicle maturation – which occurs late in cytokinesis – was incomplete in tethered cells. The wider basal connection between tethered daughters (brackets in parasites 2 and 4 in Fig. 5B–E and inset for D) contrasts with the narrow basal connection seen between individual tachyzoites (arrows in parasites 1 and 3, Fig. 5B,C).

Journal of Cell Science

Journal of Cell Science (2016) 129, 3320-3331 doi:10.1242/jcs.185223

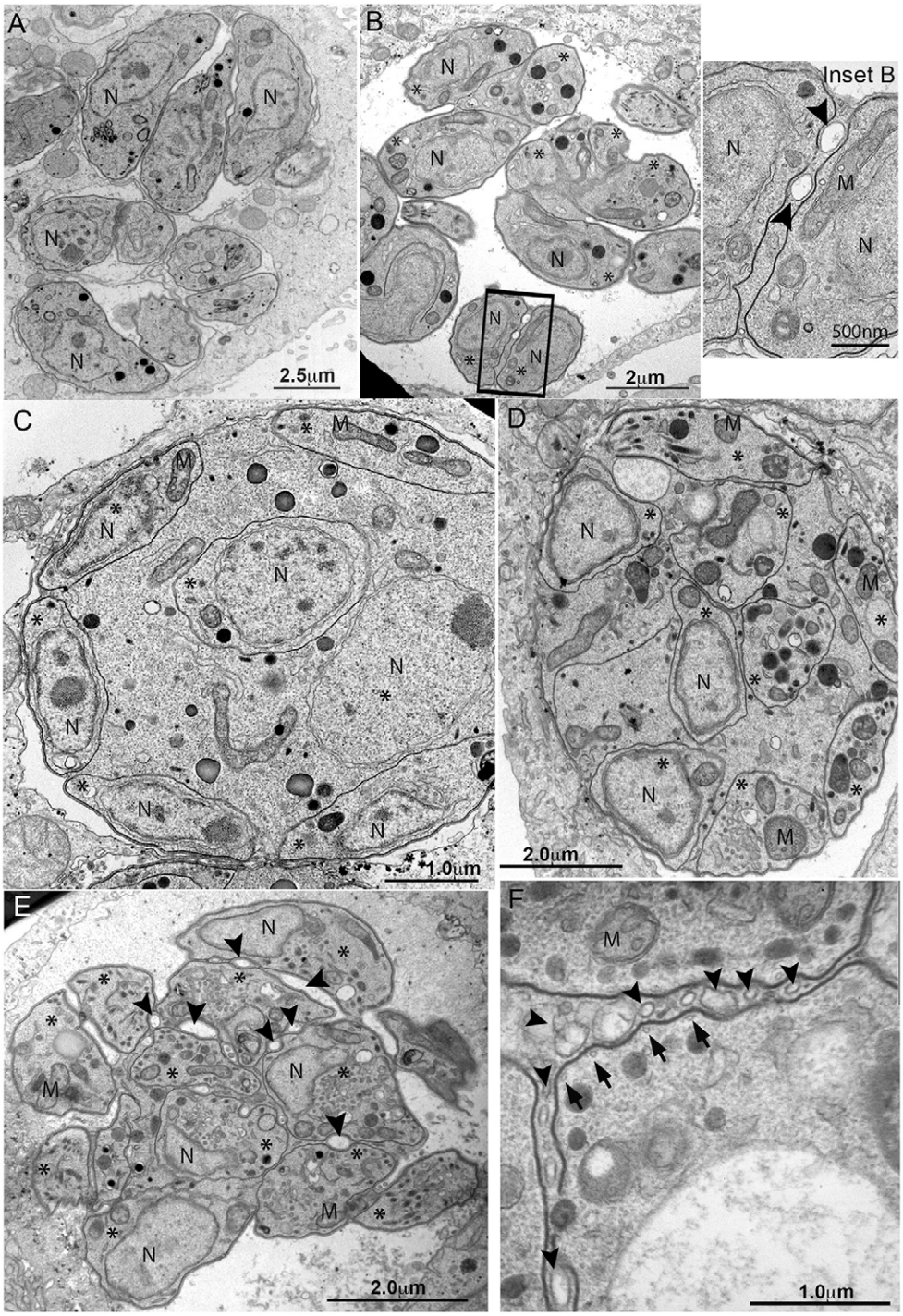

Fig. 4. TEM analysis of *T. gondii* cell division after induction of ΔACP/ACPi. (A) Non-induced tachyzoites had a normal morphology and division, whereas induction of the ΔACP/ACPi mutation for 48 h (B, with inset position indicated by a rectangle), 72 h (C) and 96 h (D–F) led to tachyzoite cytokinesis failure and the formation of masses of tethered daughter cells (asterisks) inside parasitophorous vacuoles. Although division was incomplete after induction, tethered daughter cells displayed normal morphology, including the underlying microtubules (arrows in F). Vesicles suggestive of abortive cleavage furrows were also present between daughters (arrowheads in B, E and F).
M, mitochondrion; N, nucleus.

As seen in individual parasites (circled area in Fig. 5, inset for B), tethered parasites also had a constricted posterior IMC gap (arrowhead), with thick IMC tips surrounded by an electron-dense region (circled area in insets for Fig. 5B,D). The increased electron density adjacent to the terminal end of the IMC is due to the presence of components of the basal complex, a cytoskeletal structure that caps the posterior end of the parasite (Hu, 2008; Anderson-White et al., 2011, 2012). The constriction at the basal region of daughter cells, together with the assembly of the basal complex, is a hallmark of the maturation of daughter cells, which are then ready for budding from the mother cell (Hu, 2008; Anderson-White et al., 2011).

ACP knockdown resulted in the formation of tethered daughter cells with similar morphology to that of cells treated with triclosan (Movie 2; Fig. 6). Serial images show an infected cell with two independent vacuoles (PV1 and PV2, in Fig. 6A,B and C,D, respectively) containing tethered daughter cells. Although part of the cytoplasm of these cells was encircled by a fully formed pellicle, their basal end still contained a large section of the IMC not associated with the plasma membrane. Tethered parasites also had a constricted posterior IMC gap with thick IMC tips surrounded by an electron-dense region, reminiscent of basal complex components (Fig. 6, circled areas in insets for A–D).

Journal of Cell Science

Journal of Cell Science (2016) 129, 3320-3331 doi:10.1242/jcs.185223

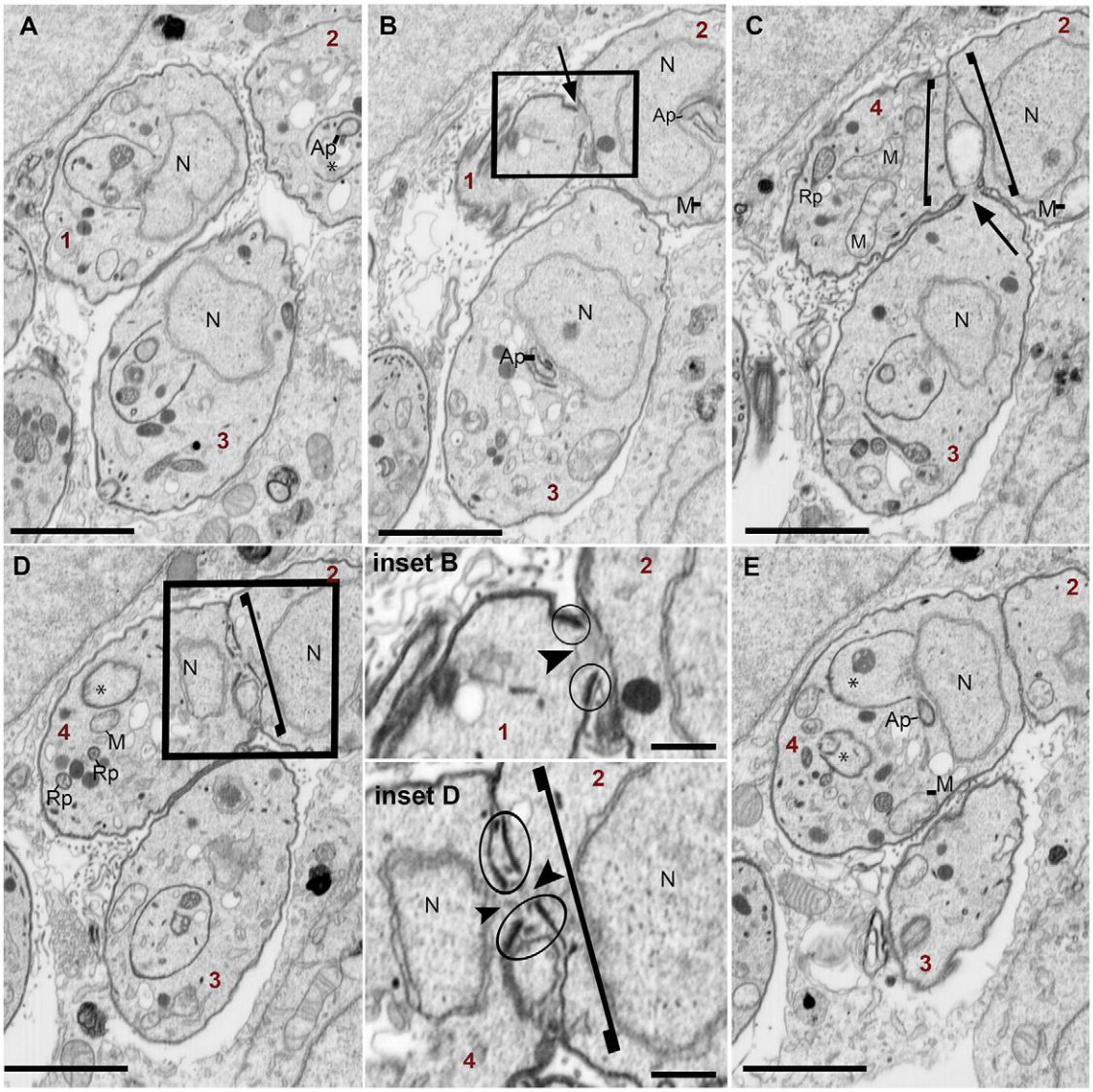

Fig. 5. Tethered daughter cells had a mature basal complex. FIB-SEM images of parasites treated with 1.0 µg/ml of triclosan for 24 h (also shown in Movie 1). (A–E) Serial images of a parasitophorous vacuole of an infected cell showing two individual parasites (1 and 3) and two tethered daughter cells (2 and 4). Tethered daughters had a wider basal connection (brackets in C and D, and inset D) compared to individual parasites (arrow in B and C). Similarly to individual parasites (circled areas in inset B), tethered parasites also showed a constricted posterior IMC gap (arrowheads in inset D) and thick electron-dense regions (ovals in inset D), showing that tethered daughter had a mature basal complex. The presence of new daughter cell scaffolds (asterisk in A,D,E) indicates that tethered daughter cells had started new rounds of division. N, nucleus; Ap, apicoplast; M, mitochondrion; Rp, ropthry. Scale bars: 2 µm (A–E); 500 nm (insets).

Thus, the overall architecture of the basal end of tethered daughters suggests that these cells reached the end of their maturation process, but that pellicle formation was incomplete, which resulted in a budding failure late in cytokinesis. Once tethered daughter cells were mature, they were able to start new rounds of division, as indicated by the presence of new daughter scaffolds in the cytoplasm (asterisks in Fig. 5A–E) and a mass containing four fully formed tethered daughter cells (PV2 in Fig. 6).

Tethered daughter cells resulted from FASII ablation have a mature partial pellicle

To confirm that the cytokinesis failure due to triclosan treatment and ACP knock down was caused by defects in the completion of pellicle assembly in emerging daughter cells, we labeled treated parasites with an antibody against the glideosome-associated protein 45 (GAP45). GAP45 is targeted to the pellicle late in cytokinesis, during pellicle maturation (the assembly of plasma membrane to the IMC) (Gaskins et al., 2004; Frénal et al., 2010). Owing to its late targeting to the membrane, GAP45 is a useful marker to study the final stages of pellicle assembly of daughter cells (Fig. 7).

At earlier stages in daughter cell assembly, only the mother cell pellicle is stained for GAP45 (Fig. 7A). However, once daughter cells reach maturity and emerge from the mother cell remnant, GAP45 colocalizes with the daughter cell IMC, indicating pellicle maturation in the regions showing colocalization (Fig. 7B). In contrast, tethered daughter cells observed after treatment with triclosan for 24 h (Fig. 7C,D) and ACP knockdown had only partial GAP45 coverage (Fig. S2). Although the outer surfaces of daughter cells were contoured with GAP45, no staining for GAP45 was

Journal of Cell Science

Journal of Cell Science (2016) 129, 3320-3331 doi:10.1242/jcs.185223

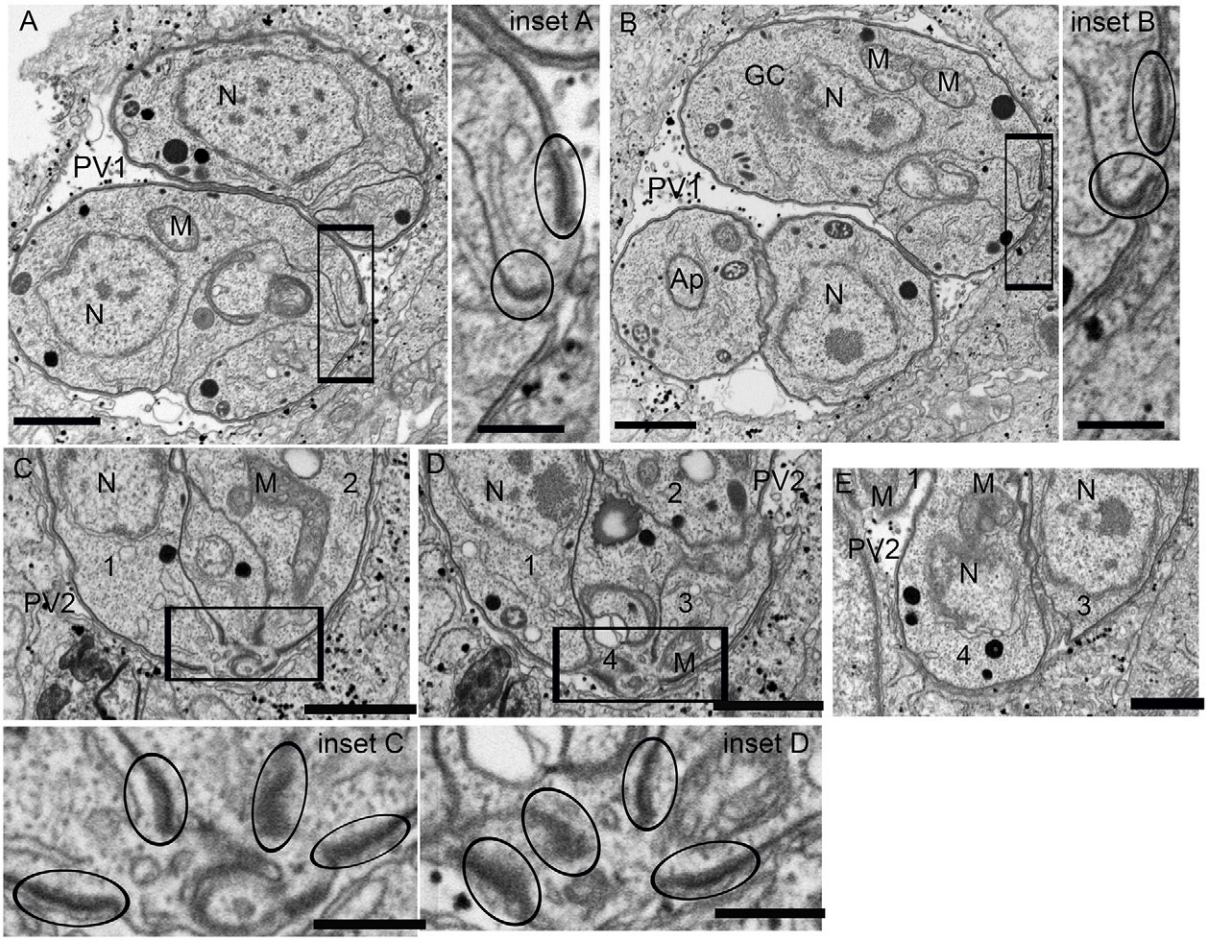

Fig. 6. Tethered daughter cells after ACP knockdown also had a mature basal complex. FIB-SEM images of ΔACP/ACPi parasites induced with Atc for 72 h (also shown in Movie 2). (A–E) Serial images of an infected cell containing two parasitophorous vacuoles with two tethered daughter cells (PV1 in A,B) and a mass of four tethered daughter cells (PV2 in C–E). Tethered parasites also had a constricted posterior IMC gap and thick electron-dense regions (ovals in insets A–D), showing that tethered daughters had a mature basal complex. N, nucleus; Ap, apicoplast; M, mitochondrion; GC, Golgi complex. Scale bars: 1 µm (A–E); 250 nm (insets).

observed on daughter IMCs localized inside the mother cell cytoplasm (arrowhead, Fig. 7C and Fig. S2). We also observed tethered daughter cells undergoing a new cycle of division while displaying only the outer pellicle labeled with GAP45 (Fig. 7D).

Long chain fatty acid supplementation rescues the cytokinesis and proliferation defects of FASII inhibition

To verify whether the lack of FASII products was the direct cause of the parasite division defect observed after triclosan treatment and ACP knockdown, we supplemented the growth medium with the main FASII products C14:0 and C16:0 (separately or as a mixture), and also with C18:1, C20:1 and C22:1 (individually), which are synthetized by the endoplasmic reticulum ELO pathway using FASII C16:0 as precursor (Ramakrishnan et al., 2012).

Quantification by fluorescent microscopy showed that supplementation with 80 µM of C14:0, C16:0, C18:1 and C22:1 (individually), and a mixture of C14:0 and C16:0 partially reverted the tachyzoite division defect, resulting in a decrease in the number of vacuoles with tethered daughter cells, after treatment with different concentrations of triclosan (Fig. 8A) and ACP knockdown induced by Atc for 48 h (Fig. 8B). Complementation with fatty acids also rescued the parasite proliferation defect, as observed by the formation of more numerous and larger plaques than those found in infected cultures not supplemented with fatty acids during treatment with 1.0 µg/ml of triclosan for 7 days (Fig. S3A) after ACP knockdown by Atc induction for 10 days (Fig. S3B).

Supplementation with exogenous C14:0 was the most effective in rescuing the formation of tethered parasites, compared with C16:0, and also with a mixture of C14:0 and C16:0 (Fig. 8A,B). Addition of exogenous unsaturated fatty acids also rescued the parasite division and proliferation defects; C18:1 had similar results to the addition of C16:0. Although supplementation with C22:1 resulted in a small degree of rescue (Fig. 8A,B), this effect was significant ($P<0.05$). However, supplementation with C20:1 was significant just for triclosan treatment.

DISCUSSION

Although fatty acid synthesis via the FAS II pathway is essential for parasite survival (Mazumdar et al., 2006; Ramakrishnan et al., 2012), the exact role of the FASII pathway for parasite cell biology had not been examined. Here, we show that FASII disruption *in vitro* – by pharmacological and genetic methods – leads to a specific defect in cytokinesis, at the end of tachyzoite cell division by endodyogeny.

FASII inhibition using the antibiotic triclosan inhibited *T. gondii* proliferation at low concentrations *in vitro* (Fig. S1A), confirming

Journal of Cell Science

Journal of Cell Science (2016) 129, 3320-3331 doi:10.1242/jcs.185223

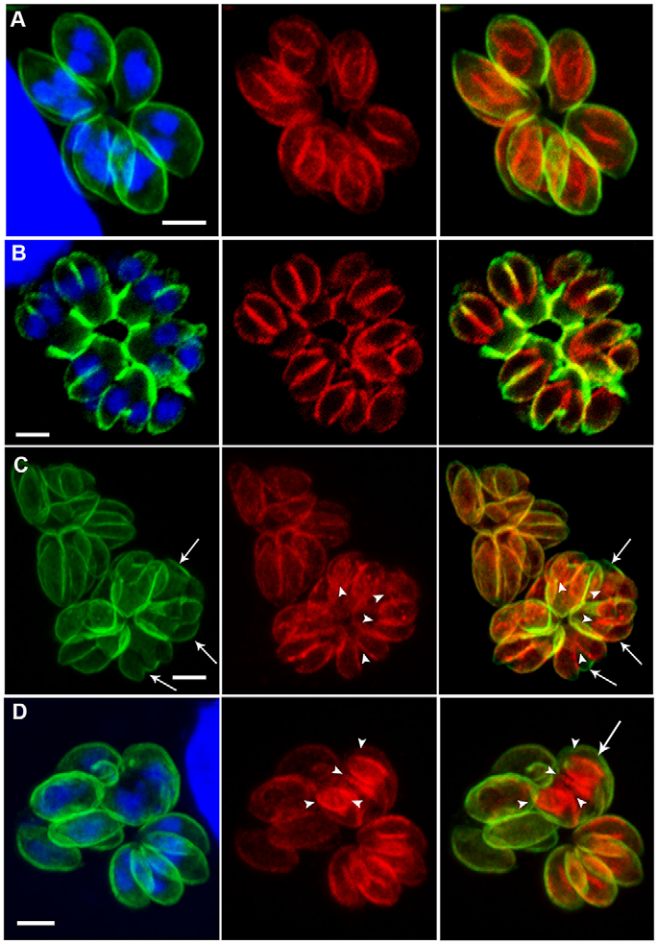

Fig. 7. Triclosan treatment affected pellicle maturation late in cytokinesis. Cells infected with *T. gondii* tachyzoites were treated with 1.0 µg/ml of triclosan for 24 h and then labeled with anti-IMC1 (in red) and anti-GAP45 (in green) antibodies, and with DAPI (DNA dye, in blue). In untreated parasites (A,B), before daughter cell maturation (A), GAP45 localizes exclusively to the mother cell pellicle of *T. gondii*; thus, it is absent from the newly formed daughter cell scaffolds, which contain IMC1. Once daughter cells reach maturity and emerge from the mother cell late at cytokinesis (B), GAP45 colocalizes to the daughter cell IMC, which indicates pellicle maturation. In contrast, after triclosan treatment (C,D), daughter cells (arrowheads) had only partial GAP45 coverage (arrows in C), this is evident in tethered daughter cells under a new cycle of division, as indicated by daughter cell scaffolds (arrowheads in D), where only the outer pellicle was labeled with GAP45 (arrow in D). Scale bars: 2 µm.

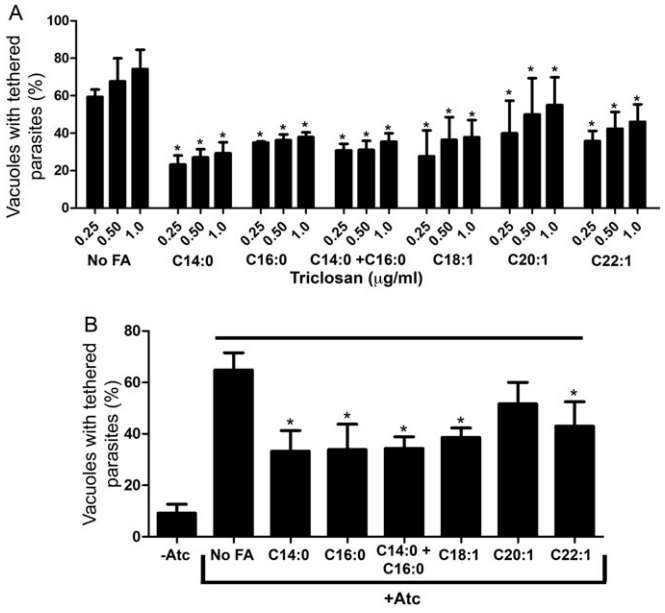

Fig. 8. Addition of exogenous fatty acids to growth medium prevents cytokinesis failure. Effect of supplementation with 80 µM of C14:0, C16:0, C18:1, C20:1 or C22:1 (separately), or with a mixture of C14:0 and C16:0 on the division of *T. gondii* tachyzoites, as measured by the number of vacuoles with tethered daughter cells after treatment of the RH strain with different concentrations of triclosan (A) or after Atc-inducible ACP knockdown in the strain ACP/ACPi (B) for 48 h. Results represent mean+s.d. of three independent experiments; **P*<0.05 compared to the 'No FA' group (no fatty acid supplementation), by two-way (A) and one-way (B) ANOVA.

that intracellular tachyzoites were sensitive to low micromolar concentrations of triclosan, as reported previously (McLeod et al., 2001). Although triclosan decreased *T. gondii* proliferation as early as 24 h after treatment initiation, plaque assays showed that, even after 5 days of treatment with 1 µg/ml of triclosan, a small number of parasites resumed proliferation, after the drug was removed from the medium (Fig. S1B–D). These data suggest that, for a small proportion of parasites, triclosan had only a static effect on cell proliferation, which was likely due to the conversion of a subpopulation of tachyzoites into drug-resistant bradyzoites, which are refractory to FASII inhibition (Fig. S1D–E). Similar results were seen after ACP knockdown (Fig. 3D). The bradyzoite stage resides in a modified parasitophorous vacuole (tissue cyst) and is responsible for the chronic phase of the disease. This stage is refractory to all available therapy against *T. gondii* (McLeod et al., 2013). Conversion into the bradyzoite stage *in vitro* can be triggered by different stress conditions, including nutrient starvation and drug pressure (Pfefferkorn et al., 1986; Dzierszinski et al., 2004; Fox et al., 2004). Thus, our results support the notion that FASII inhibition triggers stage conversion in *T. gondii*, and is ineffective against the bradyzoite stage, *in vitro*.

Morphological analysis by light and electron microscopy showed that, besides the already well-characterized apicoplast loss (Mazumdar et al., 2006), apicoplast FASII disruption also led to cytokinesis failure at the end of parasite division (Figs 1–7). Apicoplast loss by *T. gondii* seems to represent a 'signature' phenotype of the disruption of apicoplast function, both by drug treatment and by genetic disruption (Agrawal et al., 2013; Brooks et al., 2010; Fichera and Roos, 1997).

Our data suggest that FASII disruption affects not only apicoplast membrane biogenesis and maintenance, resulting in widespread apicoplast loss (Figs 1E and 3A,B), but also affects apicoplast partitioning during cell division, which would explain the presence of enlarged apicoplasts in some parasites (Fig. 1B,C; Mazumdar et al., 2006) and apicoplast missegregation (Fig. 1B).

In addition to apicoplast loss, pharmacological and genetic disruption of FASII also resulted in a parasite division defect, with incomplete daughter cell budding, at the end of cytokinesis. The cytokinesis defect was a major effect of FASII disruption, given that 45% and 71% of vacuoles contained tethered parasites after treatment with 1.0 µg/ml of triclosan for 24 h and 48 h, respectively, (Figs 1F and 8A), and 16% and 57% of ΔACP/ACPi vacuoles had tethered parasites, after 24 and 48 h of Atc treatment, respectively (Fig. 3C). The delayed effect of ACP knockdown (Fig. 3C) relative to triclosan treatment (Fig. 1F) is not surprising. Although Atc treatment inhibits ACP gene expression in ΔACP/ACPi cells, functional ACP produced before induction might persist

Journal of Cell Science

Journal of Cell Science (2016) 129, 3320-3331 doi:10.1242/jcs.185223

and maintain a functional FASII pathway. In contrast, triclosan directly inhibits the activity of a key FASII protein, and its effect is, therefore, independent of target protein turnover. However, it can't be excluded that possible off-target effects of triclosan could be also contributing to enhance the effect of this drug. The plateau observed for the ACP knockdown in the ΔACP/ACPi mutant is possibly due to the leaking of the tet-system (the expression of gene is not totally eliminated) and the resistance of bradyzoite stage to FASII disruption.

Tethered daughter cells, with the exception of apicoplast, which was absent in many tethered cells, had a completely divided nucleus and contained a complete set of organelles (Movies 1 and 2; Figs 5 and 6), including a mitochondrion (Figs 1 and 4–6), which is only incorporated into daughter cells when these are already fully mature and emerging from mother cell (Nishi et al., 2008). The presence of a constricted basal IMC (arrowheads in Fig. 5 inset D) containing an electron-dense region (circled areas in Figs 5 and 6) suggests that assembly of the basal complex – a hallmark of daughter cell maturation (Anderson-White et al., 2011) – was complete in tethered daughters. Moreover, the colocalization of the outer surface of tethered daughter cells with the glideosome component GAP45 (Fig. 7C; Fig. S2) shows that daughter cells initiated the emerging process from mother cells, assembling a mature partial pellicle. Another indication of daughter cell maturation was the fact that some tethered cells had initiated new rounds of cell division (arrowheads Fig. 2B and asterisks in Fig. 5A,D,E), which generated masses of multiple tethered daughter cells (Figs 2 and 4–6). The partial (or lack of) pellicle assembly in the inner region between daughter cells, seen by electron microscopy (Figs. 5 and 6) and by immunofluorescence microscopy for GAP45 (Fig. 7C,D; Fig. S2), suggests that FASII disruption inhibits cleavage furrow ingression and, consequently, the (*de novo*) formation of plasma membrane between daughter cells, which is essential for the assembly of the trilaminar pellicle in this region and daughter cell separation (Sheffield and Melton, 1968; Morrissette and Sibley, 2002; Agop-Nersesian et al., 2009). The delivery of new plasma membrane for furrow formation relies on the Rab11A-mediated secretory vesicle transport, which is also responsible for delivering GAP45 (Agop-Nersesian et al., 2009). Interestingly, ablation of Rab11A function results in incomplete pellicle assembly in the inner regions between daughter cells, leading to a cell separation block late in the cytokinesis, with the formation of masses of multiple daughter cells (Agop-Nersesian et al., 2009), which is similar to the phenotype of FASII disruption reported here. Overall, our combined observations suggest that tethered daughter cells resulting from FASII disruption had matured, and that the division defect exhibited by these cells represents a specific failure in assembly of the daughter cell pellicle at the final step of cytokinesis.

In a previous study, we observed a similar effect after inhibition of apicoplast DNA gyrase (Martins-Duarte et al., 2015), and hypothesized that the cytokinesis defect, in that context, could be an indirect effect of apicoplast disruption. In this work, we show that apicoplast FASII disruption is likely to be the direct cause of the cytokinesis failure, given that we observed partial recovery of parasites after addition of exogenous LCFA (C14:0 and C16:0) to the growth medium (Fig. 8 and Fig. S3). The partial recovery of parasites even when C18:1, C20:1 and C22:1 were added separately to the medium shows that lipids derived from the endoplasmic reticulum ELO system also play a role in *T. gondii* division. Apicoplast C16:0 is exported to the endoplasmic reticulum where it is modified by *T. gondii* ELOA and a stearate desaturase to form C18:1, and this lipid then is used by *T. gondii* ELOB to generate the unsaturated VLCFAs C20:1 and C22:1 (Ramakrishnan et al., 2015). VLCFA is essential for cleavage furrow ingression during cytokinesis in dividing spermatocytes of *Drosophila* (Szafer-Glusman et al., 2008). In addition, VLCFA synthesis depletion in *Arabidopsis thaliana* affected cell plate establishment late in cytokinesis, due to a delay in vesicle fusion into tubules and cell plate expansion (Bach et al., 2011). During cytokinesis, VLCFA is likely to coordinate membrane deformation and stabilize the cortical contractile components in the plasma membrane (Szafer-Glusman et al., 2008). Thus, the decrease of VLCFA synthesis after FASII disruption could also explain the lack of cleavage furrow and incomplete pellicle formation between the emerging daughter cells.

In conclusion, our results strongly suggest that FASII products and their derivatives have a fundamental role for the completion of *T. gondii* cytokinesis.

MATERIALS AND METHODS

Parasites

Toxoplasma gondii tachyzoites from the RH strain were used for the assays with triclosan, and were obtained from the peritoneal cavity of Swiss mice 2 days after infection. The experimental protocols for animal use in this study were approved by the institutional Ethics Committee for Animal Use (CEUA, IBCCF, UFRJ; approval IDs: 206-09/16) and are in agreement with the Brazilian federal law (11.794/2008, decree no. 6.899/2009).

The ΔACP/ACPi mutant strain of *T. gondii* (Mazumdar et al., 2006), kindly provided by Dr Boris Striepen from the University of Georgia (Athens, GA), was maintained *in vitro* in cultures of LLC-MK_2 cells (kidney, Rhesus monkey, *Macaca mulata*; ATCC CCL7, Rockville, MD), which were grown in RPMI medium with 5% fetal bovine serum (FBS) at 37°C and in 5% CO_2.

In vitro drug treatment assay

LLC-MK_2 cells, at a density of 5×10^5 cells, were seeded in 24-well tissue culture plates containing round coverslips in RPMI medium with 5% FBS, and were incubated for 24 h at 37°C. Then cells were infected with parasites (tachyzoites) freshly harvested from mice in RPMI without FBS, at a parasite to host-cell ratio of 10:1. Tachyzoites were allowed to interact with host cells for 30–60 min, and then cell monolayers were washed twice with medium, to remove non-adhered parasites.

After 6 h of infection, triclosan (Kumar organic products, Bangalore, India) was added to infected cultures and cells were incubated for 24 or 48 h at 37°C (assays were performed in triplicates). After treatment, cells were fixed in Bouin solution, stained with Panoptic kit solutions 2 and 3 (Laborclin Ltda, Paraná-Brazil) and observed under a light microscope. The anti-proliferative effect of triclosan on intracellular tachyzoites was estimated based on the examination of at least 1000 cells (from two different coverslips) per treatment group.

The parasite proliferation index was determined by: (the percentage of infected cells×the total number of intracellular parasites)/the total number of cells. To calculate IC_{50} values (i.e. drug concentrations that inhibit parasite growth by 50%), the percentage of parasite growth inhibition (relative to the untreated control) was plotted as a function of the drug concentration, and data were fitted to non-linear curves using Sigma Plot 8.0 (Systat Software Inc, Chicago, IL).

Plaque assay

For plaque assays, 25 cm^2 culture flasks were seeded with human foreskin fibroblasts (HFFs, ATCC) grown in high-glucose Dulbecco's modified Eagle's medium (DMEM) supplemented with 10% FBS, 2 mM L-glutamine, 100 U/ml penicillin and 100 µg/ml streptomycin (at 37°C in 5% CO_2). After cultures reached confluency, flasks were infected with 10^4 tachyzoites from the RH strain for experiments with triclosan or 10^3 tachyzoites for experiments with ΔACP/ACPi strain.

Cultures infected with RH tachyzoites were treated with 0.5 or 1.0 µg/ml of triclosan for a different number of days, according to the experiment. Cultures infected with ΔACP/ACPi were cultivated with or without 0.7 µM

of anhydrous tetracycline (Atc; Sigma-Aldrich, St Louis, MO). After triclosan treatment or knockdown induction (using Atc), cells were fixed with 100% ethanol and stained (with Panoptic kit solutions).

Immunofluorescence microscopy

LLC-MK_2 cultures were infected with tachyzoites from the RH or ΔACP/ACPi strain as described above (see '*In vitro* drug treatment assay'). Cells infected with the RH strain were treated with 0.5 or 1.0 µg/ml of triclosan for 24 and 48 h, whereas those infected with ΔACP/ACPi parasites were incubated with Atc for 24–96 h. After treatment, infected cells were fixed in 3.7% freshly prepared formaldehyde, permeabilized with 0.5% Triton X-100 for 15 min, and incubated with 50 mM NH_4Cl, for 30 min. Then samples were blocked with 3% bovine serum albumin (BSA; Sigma-Aldrich) in PBS (pH 7.2) for 1 h, and incubated for 1 h at room temperature with one of the following antibodies: rabbit polyclonal anti-SAG1 (1:1000; kindly provided by Dr John Boothroyd, University of Stanford, CA); rabbit polyclonal anti-HSP60 (1:2000; kindly provided by Dr Boris Striepen), mouse monoclonal anti-IMC1 (1:1000; kindly provided by Dr Gary Ward, University of Vermont, VT); anti-rabbit GAP45 (1:500; Gaskins et al., 2004). Goat anti-mouse- and anti-rabbit-IgG antibodies conjugated to Alexa Fluor 546 and 488 (Molecular Probes, Life Technologies, OR) were used as secondary antibodies, at a dilution of 1:600. After antibody labeling, coverslips were stained with 1 µg/ml 4,6-diamino-2-phenylindole (DAPI; Sigma-Aldrich), and also with a lectin *Dolichos biflorus* conjugated to FITC (DBA–FITC; Sigma-Aldrich). Finally, coverslips were mounted onto slides using Prolong Gold (Life Technologies), and samples were examined on a TCSSP5 Leica laser scanning confocal microscope or on a Zeiss LSM710. Brightness and contrast adjustments were performed using Photoshop.

Transmission electron microscopy

LLC-MK_2 cultures infected with tachyzoites and treated as described above were fixed with 2.5% glutaraldehyde in 0.1 M sodium cacodylate buffer (pH 7.4) and post-fixed for 45 min in the dark in 1% osmium tetroxide, 1.25% potassium ferrocyanide and 5 mM $CaCl_2$, in 0.1 M sodium cacodylate buffer (pH 7.4). Then, samples were dehydrated in acetone solutions of increasing concentrations (30–100%) and embedded in PolyBed resin (Polyscience Inc., Warrington, PA) using flat-embedding molds (EMS, Hatfield, PA). Ultrathin sections were stained with uranyl acetate and lead citrate, and observed in a Zeiss 900 (Carl Zeiss, Inc. Germany) or Jeol 1200 EX (Jeol LTD, Tokyo, Japan) transmission electron microscope.

Focused ion beam scanning electron microscopy

For observation by FIB-SEM, samples were prepared as described above (see 'Transmission electron microscopy'), and TEM sample blocks were trimmed to a pyramidal shape using a razor blade, to generate block faces of ~2 mm^2. Blocks were then mounted on aluminum support stubs, and imaged in a Helios 200 NanoLab dual-beam microscope (FEI Company, Eindhoven, NL), equipped with a gallium ion source (for focused-ion beam milling) and a field emission gun scanning electron microscope with an in-lens secondary electron detector (for imaging). Prior to imaging, a 3-nm layer of platinum was deposited onto the sample, within the microscope chamber. Milling was performed at a 30-kV acceleration voltage and a beam current of 2500 pA, in the SE imaging mode. After each milling step (slice thickness=20 nm), samples were imaged at a 2 kV acceleration voltage, 800 pA beam current and 300 ns dwell time, in 'immersion lens' mode. Image stacks and videos were generated using ImageJ (Schneider et al., 2012).

Fatty acid supplementation

Stock solutions of 100 mM of C14:0, C16:0, C18:1, C20:1 and C22:1 fatty acids (Sigma-Aldrich) were made in ethanol. Aliquots of fatty acids were dried under nitrogen and then dissolved in a sterile solution of 0.5 mM fatty acid-free BSA (Sigma-Aldrich) in PBS to obtain a fatty-acid:BSA molar ratio of 1:1. Fatty acids were added to infected cultures of LLC-MK_2 for a final concentration of 80 µM, and then parasites were allowed to grow for 48 h in the presence or absence of 0.25, 0.5 or 1.0 µg/ml triclosan for the RH strain or 0.7 µM Atc for ΔACP/ACPi. For the plaque assay, RH and ΔACP/ACPi strain parasites were incubated for 7 days in the presence of 1.0 µg/ml triclosan or 10 days in the presence of 0.7 µM Atc.

Statistical analysis

The statistical analyses were performed using Graphpad prism 5.0.

Acknowledgements

The authors thank Luis Sergio (Inmetro) and Daniel Gonçalves (Cenabio) for technical assistance with FIB-SEM microscopy and Ricardo Vilela (Inmetro) for technical assistance with the confocal microscopy. We also thank Boris Striepen for giving us the mutant ΔACP/ACPi.

Competing interests

The authors declare no competing or financial interests.

Author contributions

E.S.M.-D., R.C.V., N.S. and W.d.S. contributed to the study design. E.S.M.-D. and M.C. performed the experiments. R.C.V. helped with the experiments. E.S.M.-D. performed data analysis and interpretation. E.S.M.-D. and W.d.S. wrote the article.

Funding

This work was supported by the Indo-Brazil Collaborative Programme, sponsored by the Department of Science and Technology, Ministry of Science and Technology (India) [grant number DST/ INT/ BRAZIL RPO-01/2009/P-1] and Conselho Nacional de Desenvolvimento Científico e Tecnológico (CNPq) [grant number 490440/2009-6]; and also by fellowships and grants from CNPq, Coordenação de Aperfeiçoamento de Pessoal de Nível Superior (CAPES) and Fundação Carlos Chagas Filho de Amparo à Pesquisa do Estado do Rio de Janeiro (FAPERJ).

Supplementary information

Supplementary information available online at
http://jcs.biologists.org/lookup/doi/10.1242/jcs.185223.supplemental

References

Agop-Nersesian, C., Naissant, B., Ben Rached, F., Rauch, M., Kretzschmar, A., Thiberge, S., Menard, R., Ferguson, D. J. P., Meissner, M. and Langsley, G. (2009). Rab11A-controlled assembly of the inner membrane complex is required for completion of apicomplexan cytokinesis. *PLoS Pathog.* **5**, e1000270.

Agrawal, S., Chung, D.-W. D., Ponts, N., van Dooren, G. G., Prudhomme, J., Brooks, C. F., Rodrigues, E. M., Tan, J. C., Ferdig, M. T., Striepen, B. et al. (2013). An apicoplast localized ubiquitylation system is required for the import of nuclear-encoded plastid proteins. *PLoS Pathog.* **9**, e1003426.

Anderson-White, B. R., Ivey, F. D., Cheng, K., Szatanek, T., Lorestani, A., Beckers, C. J., Ferguson, D. J. P., Sahoo, N. and Gubbels, M.-J. (2011). A family of intermediate filament-like proteins is sequentially assembled into the cytoskeleton of *Toxoplasma gondii*. *Cell. Microbiol.* **13**, 18-31.

Anderson-White, B., Beck, J. R., Chen, C.-T., Meissner, M., Bradley, P. J. and Gubbels, M.-J. (2012). Cytoskeleton assembly in Toxoplasma gondii cell division. *Int. Rev. Cell Mol. Biol.* **298**, 1-31.

Bach, L., Gissot, L., Marion, J., Tellier, F., Moreau, P., Satiat-Jeunemaître, B., Palauqui, J.-C., Napier, J. A. and Faure, J.-D. (2011). Very-long-chain fatty acids are required for cell plate formation during cytokinesis in Arabidopsis thaliana. *J. Cell Sci.* **124**, 3223-3234.

Bisanz, C., Bastien, O., Grando, D., Jouhet, J., Maréchal, E. and Cesbron-Delauw, M. F. (2006). Toxoplasma gondii acyl-lipid metabolism: de novo synthesis from apicoplast-generated fatty acids versus scavenging of host cell precursors. *Biochem. J.* **394**, 197-205.

Bork, S., Yokoyama, N., Matsuo, T., Claveria, F. G., Fujisaki, K. and Igarashi, I. (2003). Growth inhibitory effect of triclosan on equine and bovine Babesia parasites. *Am. J. Trop. Med. Hyg.* **68**, 334-340.

Botté, C. Y., Dubar, F., McFadden, G. I., Maréchal, E. and Biot, C. (2012). Plasmodium falciparum apicoplast drugs: targets or off-targets? *Chem. Rev.* **112**, 1269-1283.

Brooks, C. F., Johnsen, H., van Dooren, G. G., Muthalagi, M., Lin, S. S., Bohne, W., Fischer, K. and Striepen, B. (2010). The toxoplasma apicoplast phosphate translocator links cytosolic and apicoplast metabolism and is essential for parasite survival. *Cell Host Microbe.* **7**, 62-73.

Charron, A. J. and Sibley, L. D. (2002). Host cells: mobilizable lipid resources for the intracellular parasite Toxoplasma gondii. *J. Cell Sci.* **115**, 3049-3059.

Crawford, M. J., Thomsen-Zieger, N., Ray, M., Schachtner, J., Roos, D. S. and Seeber, F. (2006). Toxoplasma gondii scavenges host-derived lipoic acid despite its de novo synthesis in the apicoplast. *EMBO J.* **25**, 3214-3222.

Dubremetz, J. F. and Torpier, G. (1978). Freeze fracture study of the pellicle of an eimerian sporozoite (Protozoa, Coccidia). *J. Ultrastruct. Res.* **62**, 94-109.

Dzierszinski, F., Nishi, M., Ouko, L. and Roos, D. S. (2004). Dynamics of Toxoplasma gondii differentiation. *Eukaryot. Cell* **3**, 992-1003.

Journal of Cell Science

Ferguson, D. J. P. and Hutchison, W. M. (1987). An ultrastructural study of the early development and tissue cyst formation of Toxoplasma gondii in the brains of mice. *Parasitol. Res.* **73**, 483-491.
Ferguson, D. J. P., Henriquez, F. L., Kirisits, M. J., Muench, S. P., Prigge, S. T., Rice, D. W., Roberts, C. W. and McLeod, R. L. (2005). Maternal inheritance and stage-specific variation of the apicoplast in Toxoplasma gondii during development in the intermediate and definitive host. *Eukaryot. Cell* **4**, 814-826.
Fichera, M. and Roos, D. S. (1997). A plastid organelle as a drug target in apicomplexan parasites. *Nature.* **390**, 407-409.
Fox, B. A., Gigley, J. P. and Bzik, D. J. (2004). Toxoplasma gondii lacks the enzymes required for de novo arginine biosynthesis and arginine starvation triggers cyst formation. *Int. J. Parasitol.* **34**, 323-331.
Frénal, K., Polonais, V., Marq, J.-B., Stratmann, R., Limenitakis, J. and Soldati-Favre, D. (2010). Functional dissection of the apicomplexan glideosome molecular architecture. *Cell Host Microbe* **8**, 343-357.
Gaskins, E., Gilk, S., DeVore, N., Mann, T., Ward, G. and Beckers, C. (2004). Identification of the membrane receptor of a class XIV myosin in *Toxoplasma gondii*. *J. Cell Biol.* **165**, 383-393.
Goldman, M., Carver, R. K. and Sulzer, A. J. (1958). Reproduction of *Toxoplasma gondii* by internal budding. *J. Parasitol.* **44**, 161-171.
Goodman, C. D. and McFadden, G. I. (2013). Targeting apicoplasts in malaria parasites. *Expert Opin. Ther. Targets* **17**, 167-177.
Goodman, C. D., Mollard, V., Louie, T., Holloway, G. A., Watson, K. G. and McFadden, G. I. (2014). Apicoplast acetyl Co-A carboxylase of the human malaria parasite is not targeted by cyclohexanedione herbicides. *Int. J. Parasitol.* **44**, 285-289.
Heath, R. J. and Rock, C. O. (1995). Enoyl-acyl carrier protein reductase (fabI) plays a determinant role in completing cycles of fatty acid elongation in Escherichia coli. *J. Biol. Chem.* **270**, 26538-26542.
Heath, R. J., Yu, Y.-T., Shapiro, M. A., Olson, E. and Rock, C. O. (1998). Broad spectrum antimicrobial biocides target the FabI component of fatty acid synthesis. *J. Biol. Chem.* **273**, 30316-30320.
Hu, K. (2008). Organizational changes of the daughter basal complex during the parasite replication of Toxoplasma gondii. *PLoS Pathog.* **4**, e10.
Kapoor, M., Mukhi, P. L. S., Surolia, N., Suguna, K. and Surolia, A. (2004). Kinetic and structural analysis of the increased affinity of enoyl-ACP (acyl-carrier protein) reductase for triclosan in the presence of NAD+. *Biochem. J.* **381**, 725-733.
Köhler, S., Delwiche, C. F., Denny, P. W., Tilney, L. G., Webster, P., Wilson, R. J. M., Palmer, J. D. and Roos, D. S. (1997). A plastid of probable green algal origin in Apicomplexan parasites. *Science* **275**, 1485-1489.
Martins-Duarte, E. S., Dubar, F., Lawton, P., França da Silva, C., Soeiro, M. d. N. C., de Souza, W., Biot, C. and Vommaro, R. C. (2015). Ciprofloxacin derivatives affect parasite cell division and increase the survival of mice infected with Toxoplasma gondii. *PLoS ONE* **10**, e0125705.
Mazumdar, J., Wilson, E. H., Masek, K., Hunter, C. A. and Striepen, B. (2006). Apicoplast fatty acid synthesis is essential for organelle biogenesis and parasite survival in *Toxoplasma gondii*. *Proc. Natl. Acad. Sci. USA* **103**, 13192-13197.
McLeod, R., Muench, S. P., Rafferty, J. B., Kyle, D. E., Mui, E. J., Kirisits, M. J., Mack, D. G., Roberts, C. W., Samuel, B. U., Lyons, R. E. et al. (2001). Triclosan inhibits the growth of *Plasmodium falciparum* and *Toxoplasma gondii* by inhibition of apicomplexan Fab I. *Int. J. Parasitol.* **31**, 109-113.
McLeod, R., Van Tubbergen, C., Montoya, J. G. and Petersen, E. (2013). Human toxoplasma infection. In *Toxoplasma gondii – The model Apicomplexan: Perspectives and Methods* (ed. L.M. Weiss and K. Kim), pp. 99-159. London, UK: Elsevier.
Montoya, J. G. and Liesenfeld, O. (2004). Toxoplasmosis. *Lancet* **363**, 1965-1976.
Morrissette, N. S. and Sibley, L. D. (2002). Disruption of microtubules uncouples budding and nuclear division in Toxoplasma gondii. *J. Cell Sci.* **115**, 1017-1025.
Morrissette N. S., Murray, J. M. and Roos, D. S. (1997). Subpellicular microtubules associated with an intramembranous particle lattice in the protozoan parasite Toxoplasma gondii. *J. Cell. Sci.* **110**, 35-42.
Muench, S. P., Prigge, S. T., McLeod, R., Rafferty, J. B., Kirisits, M. J., Roberts, C. W., Mui, E. J. and Rice, D. W. (2007). Studies of Toxoplasma gondii and Plasmodium falciparum enoyl acyl carrier protein reductase and implications for the development of antiparasitic agents. *Acta Crystallogr. D. Biol. Crystallogr.* **63**, 328-338.
Muñiz-Hernández, S., González del Carmen, M., Mondragón, M., Mercier, C., Cesbron, M. F., Mondragón-González, S. L., González, S. and Mondragón, R. (2011). Contribution of the residual body in the spatial organization of Toxoplasma gondii tachyzoites within the parasitophorous vacuole. *J. Biomed. Biotechnol.* **2011**, 473983.
Nishi, M., Hu, K., Murray, J. M. and Roos, D. S. (2008). Organellar dynamics during the cell cycle of *Toxoplasma gondii*. *J. Cell Sci.* **121**, 1559-1568.
Pfefferkorn, E. R., Eckel, M. and Rebhun, S. (1986). Interferon-gamma suppresses the growth of Toxoplasma gondii in human fibroblasts through starvation for tryptophan. *Mol. Biochem. Parasitol.* **20**, 215-224.
Porchet, E. and Torpier, G. (1977). Freeze fracture study of Toxoplasma and Sarcocystis infective stages. *Z. Parasitenkd.* **54**, 101-124.
Quittnat, F., Nishikawa, Y., Stedman, T. T., Voelker, D. R., Choi, J.-Y., Zahn, M. M., Murphy, R. C., Barkley, R. M., Pypaert, M., Joiner, K. A. et al. (2004). On the biogenesis of lipid bodies in ancient eukaryotes: synthesis of triacylglycerols by a Toxoplasma DGAT1-related enzyme. *Mol. Biochem. Parasitol.* **138**, 107-122.
Ramakrishnan, S., Docampo, M. D., MacRae, J. I., Pujol, F. M., Brooks, C. F., van Dooren, G. G., Hiltunen, J. K., Kastaniotis, A. J., McConville, M. J. and Striepen, B. (2012). Apicoplast and endoplasmic reticulum cooperate in fatty acid biosynthesis in apicomplexan parasite Toxoplasma gondii. *J. Biol. Chem.* **287**, 4957-4971.
Ramakrishnan, S., Docampo, M. D., MacRae, J. I., Ralton, J. E., Rupasinghe, T., McConville, M. J. and Striepen, B. (2015). The intracellular parasite Toxoplasma gondii depends on the synthesis of long-chain and very long-chain unsaturated fatty acids not supplied by the host cell. *Mol. Microbiol.* **97**, 64-76.
Schneider, C. A., Rasband, W. S. and Eliceiri, K. W. (2012). "NIH Image to ImageJ: 25 years of image analysis". *Nat. Methods* **9**, 671-675.
Sheffield, H. G. and Melton, M. L. (1968). The fine structure and reproduction of Toxoplasma gondii. *J. Parasitol.* **54**, 209-226.
Sheiner, L., Vaidya, A. B. and McFadden, G. I. (2013). The metabolic roles of the endosymbiotic organelles of Toxoplasma and Plasmodium spp. *Curr. Opin. Microbiol.* **16**, 452-458.
Surolia, N. and Surolia, A. (2001). Triclosan offers protection against blood stages of malaria by inhibiting enoyl-ACP reductase of Plasmodium falciparum. *Nat. Med.* **7**, 167-173.
Szafer-Glusman, E., Giansanti, M. G., Nishihama, R., Bolival, B., Pringle, J., Gatti, M. and Fuller, M. T. (2008). A role for very-long-chain fatty acids in furrow ingression during cytokinesis in Drosophila spermatocytes. *Curr. Biol.* **18**, 1426-1431.
Thomsen-Zieger, N., Schachtner, J. and Seeber, F. (2003). Apicomplexan parasites contain a single lipoic acid synthase located in the plastid. *FEBS Lett.* **547**, 80-86.
Van Dooren, G. G. and Striepen, B. (2013). The algal past and parasite present of the apicoplast. *Annu. Rev. Microbiol.* **67**, 271-289.
Vaughan, A. M., O'Neill, M. T., Tarun, A. S., Camargo, N., Phuong, T. M., Aly, A. S. I., Cowman, A. F. and Kappe, S. H. I. (2009). Type II fatty acid synthesis is essential only for malaria parasite late liver stage development. *Cell. Microbiol.* **11**, 506-520.
Vivier, E. and Petitprez, A. (1969). [The outer membrane complex and its development at the time of the formation of daughter cells in Toxoplasma gondii]. *J. Cell Biol.* **43**, 329-342.
Waller, R. F., Keeling, P. J., Donald, R. G. K., Striepen, B., Handman, E., Lang-Unnasch, N., Cowman, A. F., Besra, G. S., Roos, D. S. and McFadden, G. I. (1998). Nuclear-encoded proteins target to the plastid in Toxoplasma gondii and Plasmodium falciparum. *Proc. Natl. Acad. Sci. USA* **95**, 12352-12357.
Waller, R. F., Ralph, S. A., Reed, M. B., Su, V., Douglas, J. D., Minnikin, D. E., Cowman, A. F., Besra, G. S. and McFadden, G. I. (2003). A type II pathway for fatty acid biosynthesis presents drug targets in Plasmodium falciparum. *Antimicrob. Agents Chemother.* **47**, 297-301.
Welti, R., Mui, E., Sparks, A., Wernimont, S., Isaac, G., Kirisits, M., Roth, M., Roberts, C. W., Botté, C., Maréchal, E. et al. (2007). Lipidomic analysis of Toxoplasma gondii reveals unusual polar lipids. *Biochemistry.* **46**, 13882-13890.
White, S. W., Zheng, J., Zhang, Y.-M. and Rock, C. O. (2005). The structural biology of type II fatty acid biosynthesis. *Annu. Rev. Biochem.* **74**, 791-831.
Wiesner, J., Reichenberg, A., Heinrich, S., Schlitzer, M. and Jomaa, H. (2008). The plastid-like organelle of apicomplexan parasites as drug target. *Curr. Pharm. Des.* **14**, 855-871.
Williamson, D. H., Gardner, M. J., Preiser, P., Moore, D. J., Rangachari, K. and Wilson, R. J. (1994). The evolutionary origin of the 35kb circular DNA of Plasmodium falciparum: new evidence supports a possible rhodophyte ancestry. *Mol. Gen. Genet.* **243**, 249-252.
Yu, M., Kumar, T. R. S., Nkrumah, L. J., Coppi, A., Retzlaff, S., Li, C. D., Kelly, B. J., Moura, P. A., Lakshmanan, V., Freundlich, J. S. et al. (2008). The fatty acid biosynthesis enzyme FabI plays a key role in the development of liver-stage malarial parasites. *Cell. Host. Microbe.* **4**, 567-578.
Zhang, Y. W., Halonen, S. K., Ma, Y. F., Wittner, M. and Weiss, L. M. (2001). Initial characterization of CST1, a *Toxoplasma gondii* cyst wall glycoprotein. *Infect. Immun.* **69**, 501-507.
Zuther, E., Johnson, J. J., Haselkorn, R., McLeod, R. and Gornicki, P. (1999). Growth of Toxoplasma gondii is inhibited by aryloxyphenoxypropionate herbicides targeting acetyl-CoA carboxylase. *Proc. Natl. Acad. Sci. USA* **96**, 13387-13392.